

**Size control for two-dimensional iron oxide nano-dots derived from  
biological molecules**

Masato Tominaga\*, Manabu Matsumoto, Kazuki Soejima and Isao Taniguchi\*

Department of Applied Chemistry and Biochemistry,  
Faculty of Engineering, Kumamoto University, Kumamoto 860-8555, Japan

[\*] Corresponding author:

Masato Tominaga

e-mail: [masato@gpo.kumamoto-u.ac.jp](mailto:masato@gpo.kumamoto-u.ac.jp)

Tel.: +81-96-342-3656, Fax: +81-96-342-3656

## **Abstract**

We demonstrated the fabrication of size controlled two-dimensional iron oxide nano-dots derived from the heat-treatment of ferritin molecules self-immobilized on modified silicon surfaces.

Ferritin molecules were immobilized onto 3-aminopropyltrimethoxysilane (3-APMS) modified silicon surfaces by electrostatic interactions between negatively charged amino acids of ferritin molecules and amino terminal functional groups of 3-APMS. Heat-treatments were performed at 400 °C for 60 min to fabricate two-dimensional nano-dots based on ferritin cores, a heat-treatment at was performed. XPS and FT-IR results clearly indicate that ferritin shells were composed of amino acids and 3-APMS modifiers on silicon surfaces were eliminated by heat-treatment. Nano-dots on substrate surfaces corresponded to iron oxides. The size of nano-dots was tunable in the range of 0 ~ 5 ( $\pm 0.75$ ) nm by in situ reactions of iron ion chelators with ferritin molecules immobilized on substrates before heat-treatment.

**keywords:** ferritin, protein, nano-dots, iron oxide, chelator, AFM

## **1. Introduction**

Ferritin is a spherical cage-like, iron storage protein [1-6]. Ferritin is composed of 24-subunits, which form a hollow protein shell enclosing a cavity of ca. 8 nm in diameter. The outer diameter of the protein shell is 12 nm [1-6]. There are two types of ion channels lying on eight 3-fold and six 4-fold symmetry axes on the ferritin shell. 3-fold and 4-fold ion channels are hydrophilic and hydrophobic, respectively. In the cavity, up to 4500 iron atoms can be stored as hydrous ferric oxide minerals similar to the structure of ferrihydrite. The iron uptake and release mechanisms of ferritin are caused by the oxidation and reduction of iron ions (Fe(II) / Fe(III)) [1-6].

Protein engineering of viral cages for constrained nanomaterial syntheses is an attractive research field [7-23]. The formation of solids in biological systems, biomineralization, has provided inspiration for the controlled formation of inorganic materials. Ferritin, an iron-storage protein, is a potential candidate for the protein engineering of nanomaterial syntheses [11-13]. In fact, it has been reported that the formation of nanoparticles consisting of inorganic species such as iron oxide, cobalt, nickel, chromium, copper, indium and Prussian blue in the ferritin cavity [9,14-17], and the fabrication of inorganic nanoparticles derived from ferritin on substrate surface [10,18-20]. Furthermore, ferritin cores have been used as catalysts [21-23].

In the present study, we fabricated of tunable size-controlled inorganic nano-dots by the heat-treating ferritin. Size control was performed by direct *in situ* reactions of metal ion chelators with ferritin core metals immobilized on silicon surfaces. This simple and effective method is useful for fabricating size controlled nanoparticles for catalysts, biomedical sensing and other nanotechnological applications.

## **2. Materials and methods**

Horse spleen ferritin (Type I, Sigma) was purified by size exclusion chromatography [24]. The concentration of purified ferritin was determined by the BCA-protein reaction (BCA protein assay kit, PIERCE Chem. Comp., USA) against an albumin standard curve [25]. The number of iron atoms per ferritin molecule used in this study was evaluated to be approximately  $3.3 \times 10^3$  atoms by inductively coupled plasma-atomic emission and atomic absorption spectroscopies. A polished silicon wafer (5 x 5 mm) was used as a substrate for ferritin immobilization. To remove adsorbed organic contaminants on silicon surfaces, surfaces were treated by immersion into 30 % H<sub>2</sub>O<sub>2</sub>: 30% NH<sub>4</sub>OH: water (1:1:5(v/v)) for 10 min with sonication, and for 30 min at 60 °C. Silicon surfaces were washed with water several times with sonication, and finally washed with ethanol. Clean silicon surfaces were modified with 3-aminopropyltrimethoxysilane (3-APMS, AZmax Co., Japan) according to a method described in a previous paper [25]. Ferritin was immobilized onto 3-APMS modified silicon surfaces by immersion of substrates into a phosphate buffer solution (pH7,  $\mu=0.1$ ) of  $0.02 \sim 0.2 \mu\text{mol dm}^{-3}$  ferritin for 10 s. A nitrilotriacetic acid (NTA, Nacalai Tessque Co., Japan) was used as an iron ion chelator. Water was purified with a Millipore Milli-Q water system. Other reagents used in this study were of analytical grade. Tapping-mode AFM measurements were carried out under an air atmosphere.

### 3. Results and discussion

Fig. 1 shows results from X-ray photoelectron spectroscopy (XPS). Before modification with 3-aminopropyltrimethoxysilane (3-AMPS), a peak at 284.5 eV corresponding to C(1s) was observed on silicon substrates with bare silicon dioxide surfaces as shown in Fig. 1Aa). Although substrates

were kept under a clean atmosphere, the peak indicates silicon substrates were contaminated with organic species. Therefore, the C(1s) peak at the bare silicon surface was used as control data. An increase in the C(1s) peak intensity was observed after silicon surface modification with 3-APMS (Figure 1Ab), indicating 3-APMS monolayers formed on the surface. As shown in Fig. 1Bb), an XPS peak around 402 eV corresponding to N(1s) was also observed on the 3-APMS modified substrate. The N(1s) peak was not observed before the modification. These results clearly indicate that the silicon surface was modified with 3-APMS. After ferritin immobilized onto the 3-APMS modified silicon surface, a significant increase in N(1s) peak intensity was observed, clearly indicating ferritin was present on the surface. Ferritin molecules were immobilized onto 3-APMS modified surfaces by electrostatic interactions between negatively charged amino acids of ferritin molecules and amino terminal functional groups of 3-APMS. After heat-treatment at 400 °C for 60 min, the N(1s) peak was no longer present, at least below the detection limit, and the C(1s) peak intensity decreased to a peak intensity observed at control levels. These results clearly indicate that ferritin shells composed of amino acids were eliminated by heat-treatment. The elimination of 3-APMS on the surface was also indicated by XPS analyses. FT-IR analyses also supported the elimination of protein shells by heat-treatment. Before heat-treating immobilized ferritin molecules, signals at approximately 1667 and 1545  $\text{cm}^{-1}$  corresponding to amide I and II bands, respectively, were observed, which are specific for peptide bonds in protein shells. The amide band signals completely disappeared after heat-treating at 400 °C for 60 min [23].

Fig. 2 shows tapping-mode AFM images before and after ferritin immobilization onto the 3-APMS modified silicon surface. The 3-APMS modified silicon surface was significantly flat when compared to ferritin sized,  $\sim 12$  nm (Fig. 2a). As shown in Fig. 2b), the size of each ferritin molecule was evaluated to be approximately 11 ( $\pm 1.5$ ) nm in diameter in z-plane thickness, which is

comparable to the expected ~12 nm diameter determined by x-ray diffraction.[1-6] After heat-treatment at 400 °C for 60 min, two-dimensional nano-dot arrays derived from ferritin cores were observed at silicon surfaces as shown in Fig. 3a). XPS results for nano-dot arrays on the surface showed broad peaks around 712 eV corresponding to iron species. The aforementioned result together with previous reports indicate that the observed nano-dot arrays were composed of FeOOH iron oxides.[10,26,27] The size distribution of iron oxide nano-dots determined by z-plane thickness with AFM measurements is shown in Fig. 3a), which indicates the size of iron oxides was 4.75 (± 1.0) nm in diameter. The iron oxide diameter 4.75 (± 1.0) nm, is reasonable in size, since the ferritin used in this study contained approximately  $3.3 \times 10^3$  iron atoms. The previous result also supports the fact that the protein shell of ferritin was eliminated by heat-treatment.

It is known that nitrilotriacetic acid (NTA) acts as a chelator for various metals [28]. NTA complex formation with iron(III) ions is shown as follows:  $K_1 = [\text{Fe(III)(NTA)}]/([\text{Fe(III)}][\text{NTA}])$ ,  $K_2 = [\text{Fe(III)(NTA)}_2]/([\text{Fe(III)(NTA)}][\text{NTA}])$ , where  $[\text{Fe(III)}]$ ,  $[\text{NTA}]$ ,  $[\text{Fe(III)(NTA)}]$  and  $[\text{Fe(III)(NTA)}_2]$  are the concentration of iron(III) ion, NTA with dissociated carboxylic acid, (NTA)-Fe(III) and bis(NTA)-Fe(III) complexes, respectively. Complex formation constants, ( $\log K_1$ ) and ( $\log K_2$ ) are 15.9 and 23.97, respectively, at 25 °C under an ionic strength of 0.10 mol dm<sup>-3</sup> [28,29]. NTA is a powerful complexing agent as an iron chelator, especially in neutral or basic solutions. NTA would be able to diffuse into the protein cavity, because NTA is a relatively small molecule and passes through ferritin ion channels [30]. NTA diffused into the cavity would directly react with the ferritin core consisting of iron(III) ions, resulting in (NTA)-Fe(III) and/or bis(NTA)-Fe(III) complex formation. Complex formation is accelerated when ferritin core iron(III) ions are reduced to iron(II) ions by a chemical agent or electrochemical reactions [25,31,32] After ferritin immobilized onto 3-APMS modified silicon surfaces was immersed into a phosphate buffer solution

of  $10 \mu\text{mol dm}^{-3}$  NTA for 20 min, ferritin molecules immobilized onto silicon surfaces and were observed by AFM measurements. The overall shape of ferritin molecules was the same as that prior to reacting with NTA. The size of each ferritin molecule was evaluated to be approximately  $11 (\pm 1.5)$  nm in diameter in z-plane thickness, which is the same size as unreacted ferritin shown in Fig. 2b). However, after ferritin immobilized on silicon substrates was heat-treated at  $400 \text{ }^\circ\text{C}$  for 60 min, iron oxide nano-dots were observed at surfaces. Nano-dots were evaluated to be  $1.25 (\pm 0.5)$  nm in diameter as shown in Fig. 3b). Nano-dot sizes were evaluated by z-plane thickness with AFM measurements. The aforementioned result indicates that NTA formed complexes with iron(III) ions and ferritin core sizes decreased in comparison with those prior to reacting with NTA. On the other hand, some nano-dots with  $\sim 5$  nm diameters were also observed on surfaces, which were almost the same size,  $4.75 (\pm 1.0)$  nm in diameter, observed with untreated molecules. The observation of these nano-dots ( $\sim 5$  nm) indicates that, for these proteins, NTA was not able to directly react with ferritin cores. The reason why NTA could not pass through the ion channels is not clear. When reaction times were increased to 30 min, a limited number of ca. 5 nm iron nano-dots were observed as shown in Fig. 3c), indicating that almost all ferritin cores were completely removed and/or were reduced lower than the detection limit ( $\sim 0.25$  nm) in z-plane thickness. Ferritin cores, which could not react with NTA, were only present on the surface. To summarize, the plot for size distribution of nano-dots as a function of reaction time with NTA is shown in Fig. 4. Decrease in the size of nano-dots was not observed in a buffer solution in the absence of NTA in the time range ( $\sim 30$  min). The preliminary results presented herein clearly indicate that the size of iron oxide derived from ferritin cores on silicon surfaces is tunable and controlled *in situ* by reacting NTA with ferritin

molecules immobilized on silicon surfaces (Fig. 5). We are currently carrying out a more in-depth study to achieve size controlled nano-dots with a sharper size distribution.

In summary, we have demonstrated the fabrication of size controlled two-dimensional iron oxide nano-dots derived from the heat-treatment of ferritin molecules self-immobilized on modified silicon surfaces. The size of nano-dots is tunable in the range of 0 ~ 5 ( $\pm 0.75$ ) nm by *in situ* reactions of iron ion chelators with ferritin molecules. Further investigations are under way not only to achieve homogeneity in particle size, but also to investigate the effect of NTA concentration on the distribution and size of nano-dots. This simple and effective size control method is of importance for implications in the design of catalysts, biomedical sensing and other nano-technological applications.

## **Acknowledgments**

This work was supported by a Grant-in-Aid for Scientific Research (M.T.) from the Ministry of Education, Culture, Science, Sports and Technology, Japan. M.T. acknowledges Iketani Science and Technology Foundation.

## **References**

- [1] P. M. Harrison, T. H. Lilley, in: T. M. Loehr (Eds.), *Iron Carriers and Iron Proteins*, VCH, New York, 1989, Ch. 2.
- [2] T. G. St. Pierre, P. Chan, K. R. Bauchspiess, J. Webb, S. Betteridge, S. Walton, D. P. E. Dickson, *Coord. Chem. Rev.* 151 (1996) 125.



- [3] P. M. Proulx-Curry, N. D. Chasteen, *Coord. Chem. Rev.* 144 (1995) 347.
- [4] G. D. Watt, R. B. Frankel, G. C. Papaefthymiou, *Proc. Natl. Acad. Sci.* 82 (1985) 3640.
- [5] P. M. Harrison, P. J. Artymiuk, G. C. Ford, D. M. Lawson, J. M. A. Smith, A. Treffry, J. L. White, in: S. Mann, J. Webb, R. J. P. Williams (Eds.), *Biom mineralization Chemical and Biochemical Perspectives*, Wiley-VCH, Weinheim, 1989, Ch. 9.
- [6] X. Liu, E. C. Theil, *Acc. Chem. Res.* 38 (2005) 167.
- [7] T. Douglas, E. Strable, D. Willits, A. Aitouchen, M. Libera, M. Yound, *Adv. Mater.* 14 (2002) 415.
- [8] M. Allen, D. Willits, J. Mosolf, M. Young, T. Douglas, *Adv. Mater.* 14 (2002) 1562.
- [9] T. Douglas, V. T. Stark, *Inorg. Chem.* 39 (2002) 1828.
- [10] I. Yamashita, *Thin Solid Films* 393 (2001) 12.
- [11] S. C. Tsang, J. Qiu, P. J. F. Harris, Q. J. Fu, N. Zhang, *Chem. Phys. Lett.* 322 (2000) 553.
- [12] J.-M. Bonard, P. Chauvin, C. Klinke, *Nano Lett.* 6 (2002) 665.
- [13] Y. Zhang, Y. Li, W. Kim, D. Wang, H. Dai, *App. Phys. A* 74 (2002) 325.
- [14] M. Okuda, K. Iwahori, I. Yamashita, H. Yoshimura, *Biotech. Bioeng.* 84 (2003) 187.
- [15] J. M. Dominguez-Vera, E. Colacio, *Inorg. Chem.* 42 (2003) 6983.
- [16] D. Ensign, M. Young, T. Douglas, *Inorg. Chem.* 43 (2004) 3441.
- [17] M. Tominaga, L. Han, L. Wang, M. M. Maye, J. Luo, N. Kariuki, C. J. Zhong, *J. Nanosci. Nanotech.* 4 (2004) 708.
- [18] H.-A. Hosein, D. R. Strongin, M. Allen, T. Douglas, *Langmuir* 20 (2004) 10283.
- [19] M. Okuda, Y. Kobayashi, K. Suzuki, K. Sonoda, T. Kondoh, A. Wagawa, A. Kondo, H. Yoshimura, *Nano Lett.* 5 (2005) 991.
- [20] S. Yoshii, K. Yamada, N. Matsukawa, I. Yamashita, *Jpn. J. Appl. Phys.* 44 (2005) 1518.

- [21] Y. Li, W. Kim, Y. Zhang, M. Rolandi, D. Wang, H. Dai, *J. Phys. Chem. B* 105 (2001) 11424.
- [22] T. Ueno, M. Suzuki, T. Goto, T. Matsumoto, K. Nagayama, Y. Watanabe, *Angew. Chem. Int. Ed.* 43 (2004) 2527.
- [23] M. Tominaga, A. Ohira, A. Kubo, I. Taniguchi, M. Kunitake, *Chem. Commun.* 2004, 1518.
- [24] P. K. Smith, R. I. Krohn, G. T. Hermanson, A. K. Mallia, F. H. Gartner, M. D. Provenzano, E. K. Fujimoto, N. M. Goeke, B. J. Olson, D. C. Klenk, *Anal. Biochem.* 150 (1985) 76.
- [25] M. Tominaga, K. Soejima, M. Manabu, I. Taniguchi, *J. Electroanal. Chem.* 579 (2005) 51.
- [26] T. Hikono, Y. Uraoka, T. Fuyuki, I. Yamashita, *Jpn. J. Appl. Phys.* 42 (2003) L398.
- [27] K. C. Martin, S. M. Villano, P. R. McCurdy, D. C. Zapien, *Langmuir* 19 (2003) 5808.
- [28] Dissociation constants,  $pK_{a1}$ ,  $pK_{a2}$  and  $pK_{a3}$ , for carboxylic acids of NTA are 1.72, 2.52 and 9.70, respectively, at 25 °C under an ionic strength of 0.10 mol dm<sup>-3</sup>.
- [29] L. G. Sillen, A. E. Martell, *Stability Constants*, The Chemical Society, London, 1964; E. HXgfeldt, D. D. Perrin, *Stability Constants of Metal-Ion Complexes*, Pergamon, Oxford, 1979.
- [30] X. Yang, N. D. Chasteen, *Biophys. J.* 71 (1996) 1587.
- [31] T. D. Martin, S. A. Monheit, R. J. Niichel, S. C. Peterson, C. H. Campbell, D. C. Zapien, *J. Electroanal. Chem.* 420 (1997) 279.
- [32] M. Tominaga, A. Ohira, Y. Yamaguchi, M. Kunitake, *J. Electroanal. Chem.* 566 (2004) 323.

### Figure captions

Fig. 1. XPS spectra in C(1s) (A) and N(1s) (B) regions for bare silicon substrate surfaces (a), silicon surfaces after modification with 3-APMS (b), 3-APMS modified surfaces after

immobilization of ferritin (c), and the ferritin immobilized surface after heat-treatment at 400 °C for 60 min (d).

Fig. 2. Tapping-mode AFM images for silicon surfaces modified with 3-APMS (a) and ferritin molecules immobilized onto the 3-APMS modified silicon surface. The cross-sectional view corresponds to the line drawn.

Fig. 3. Tapping-mode AFM images for the iron oxide nano-dot derived from heat-treatment at 400 °C for 60 min for ferritin immobilized onto substrate surfaces. Immobilized ferritin molecules on modified substrates were reacted with a phosphate buffer solution (pH 7,  $\mu=0.1$ ) of  $10 \mu\text{mol dm}^{-3}$  NTA at room temperature for 0 (a), 20 (b), and 30 (c) min. Size distributions for iron oxide nano-dot by analysis in z-plane thickness are shown. Unreacted ferritin core with NTA was not counted in size distributions.

Fig. 4. Size-controlled iron oxide nano-dot as a function of reaction time on  $10 \mu\text{mol dm}^{-3}$  NTA in a phosphate buffer solution (pH 7,  $\mu=0.1$ ).

Fig. 5. The scheme for fabrication of size-controlled iron oxide nano-dot derived from ferritin on substrate surfaces.

## Graphical contents

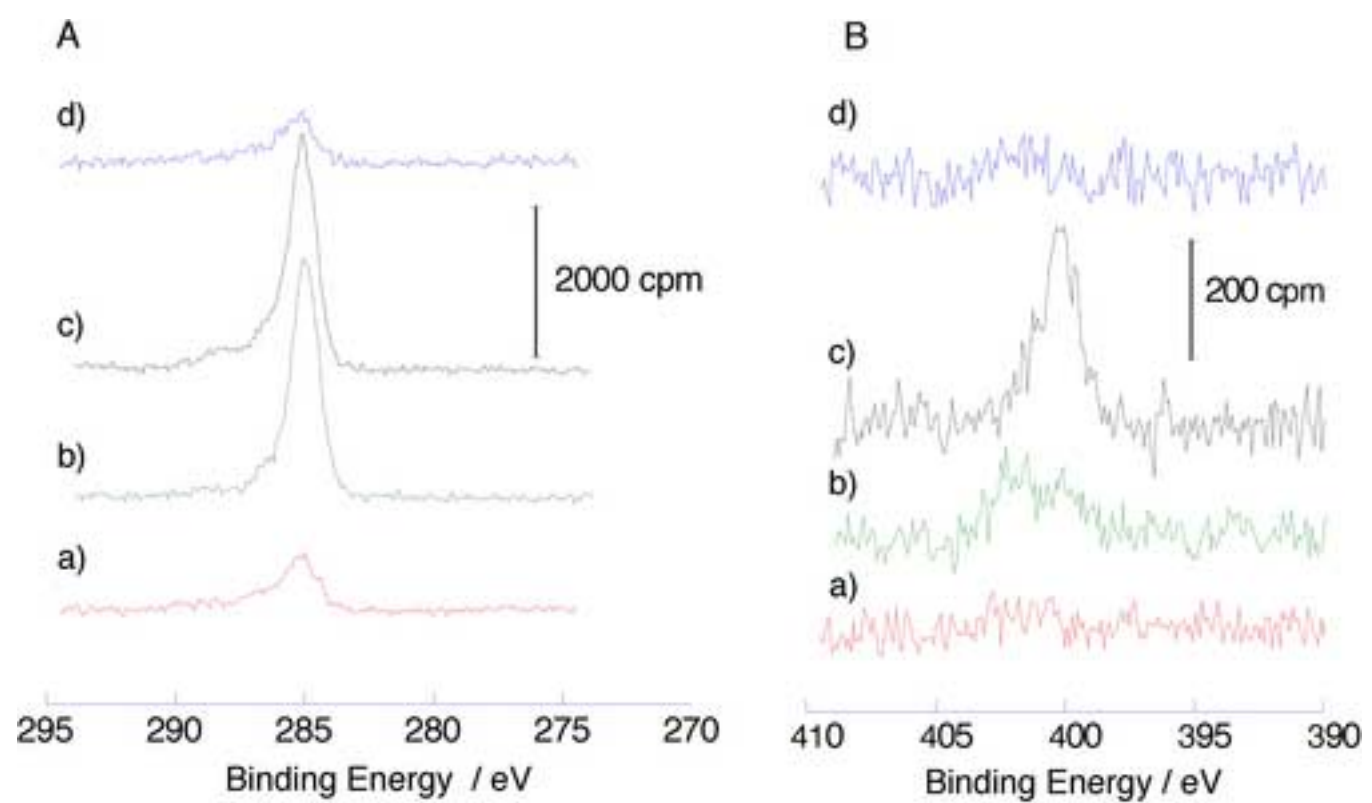


Fig. 1

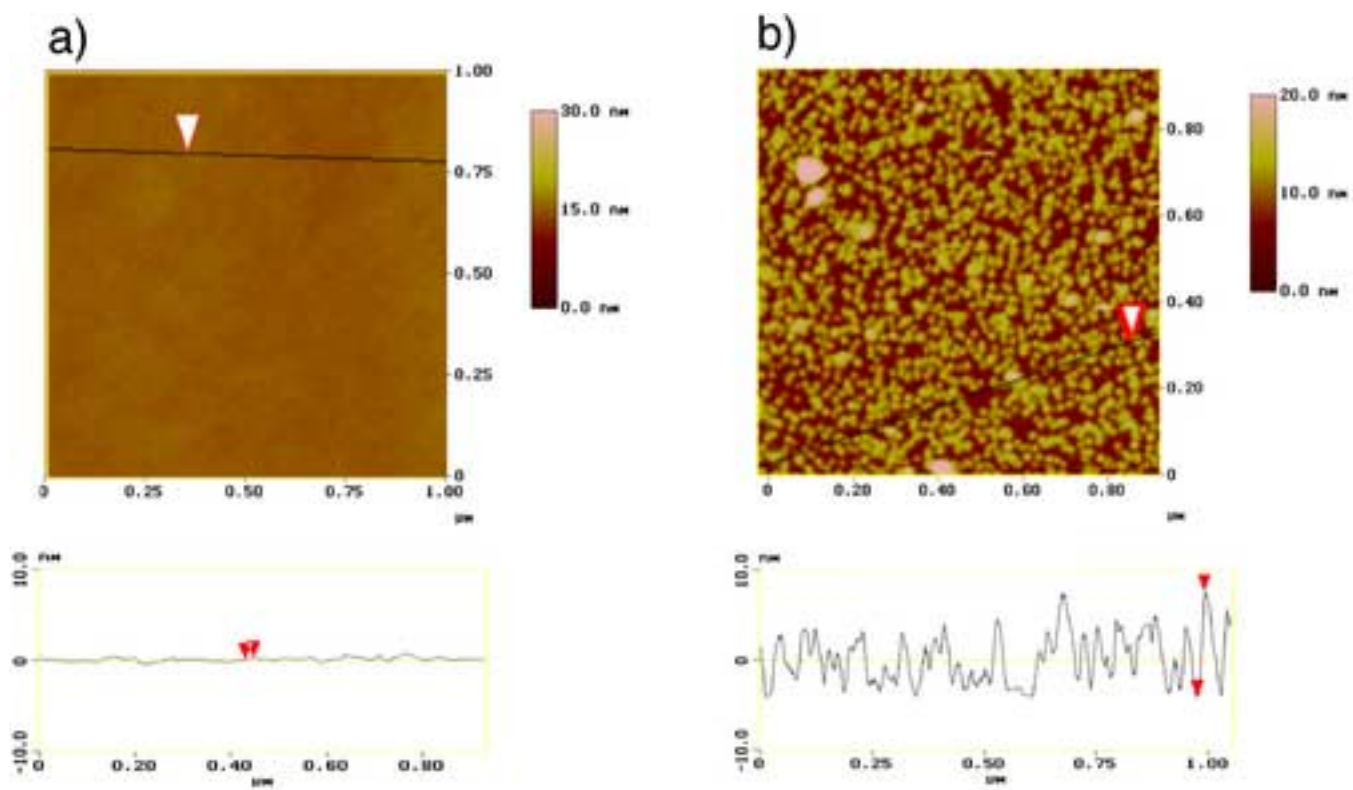


Fig. 2

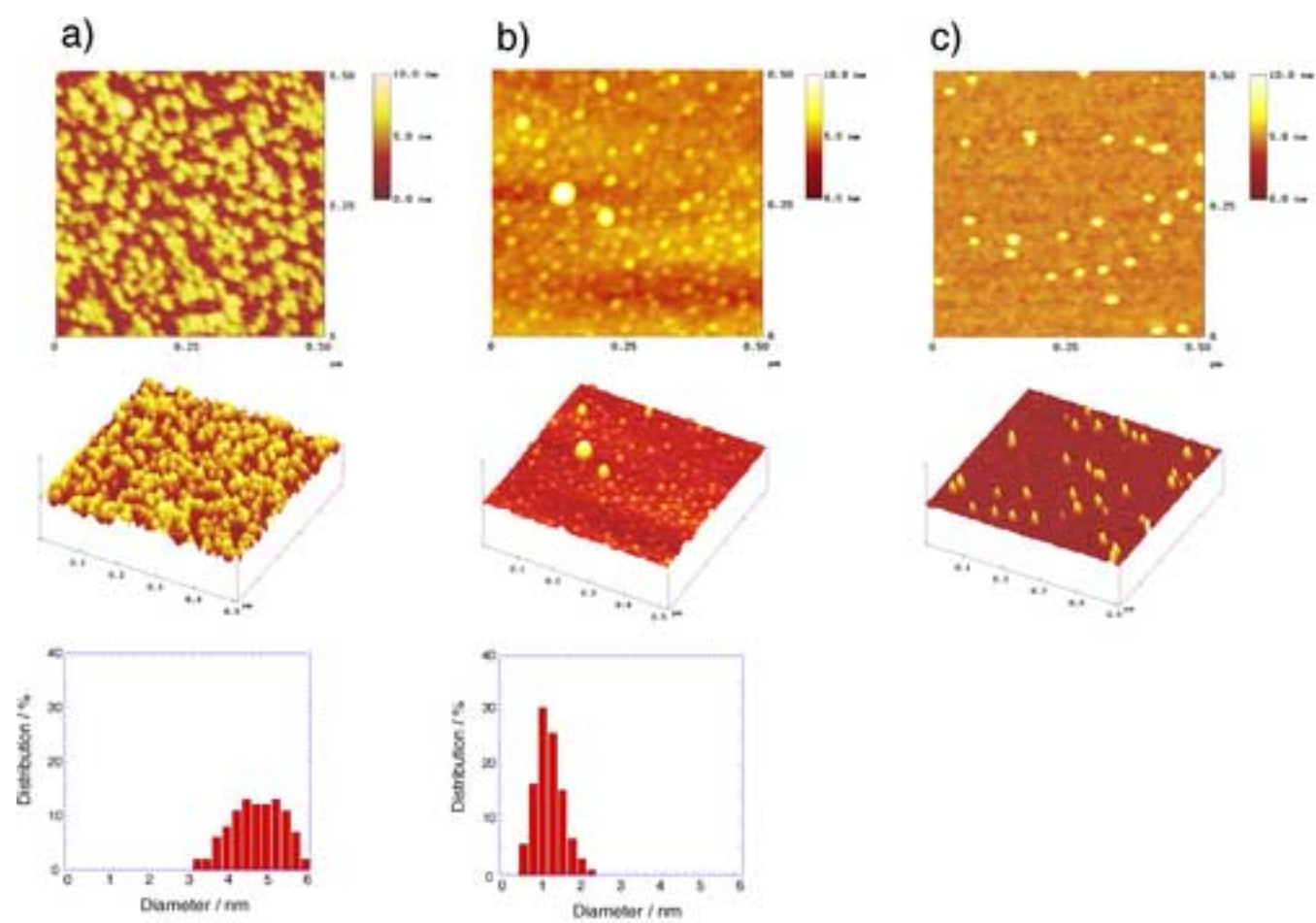


Fig. 3

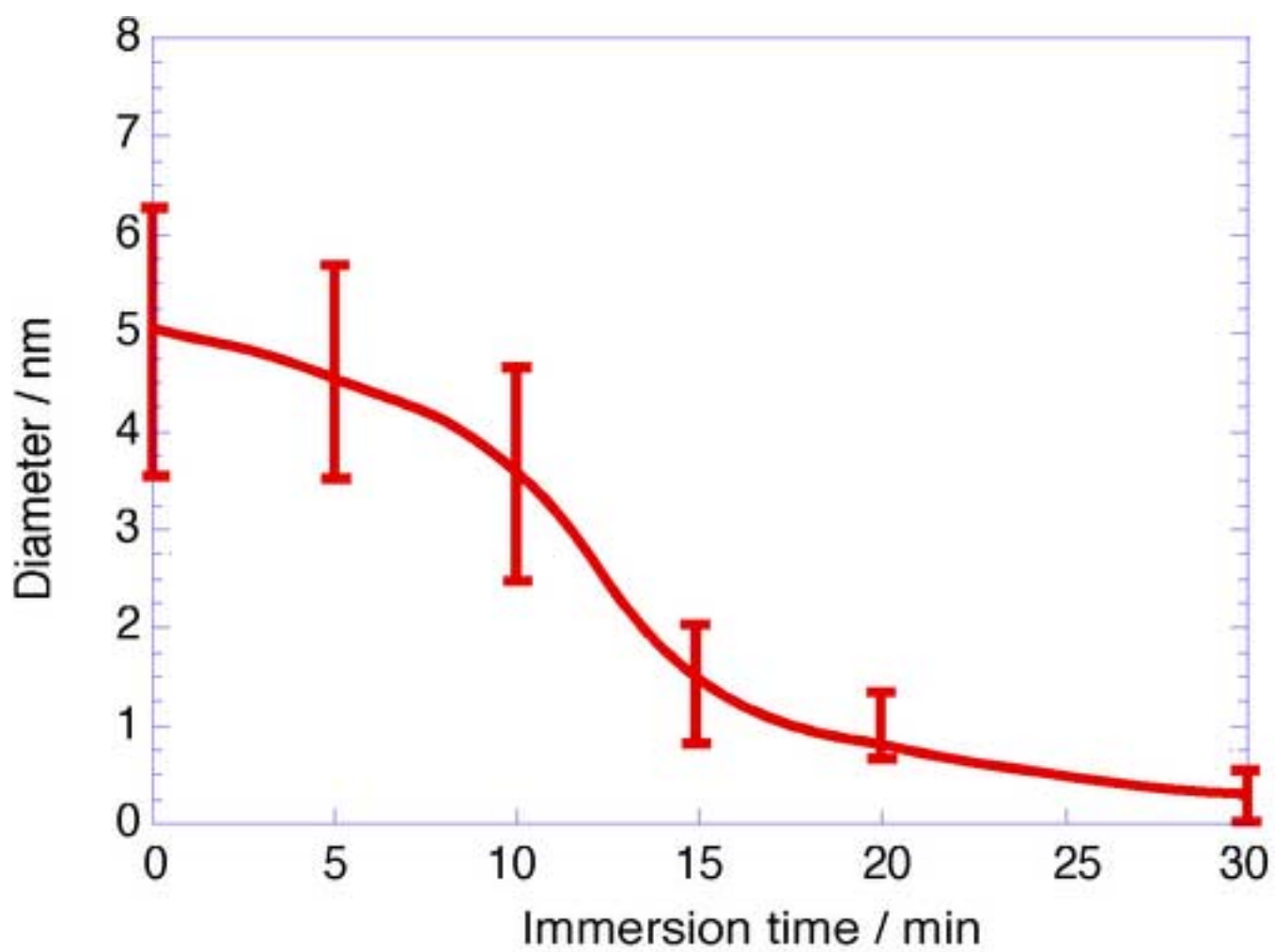


Fig. 4

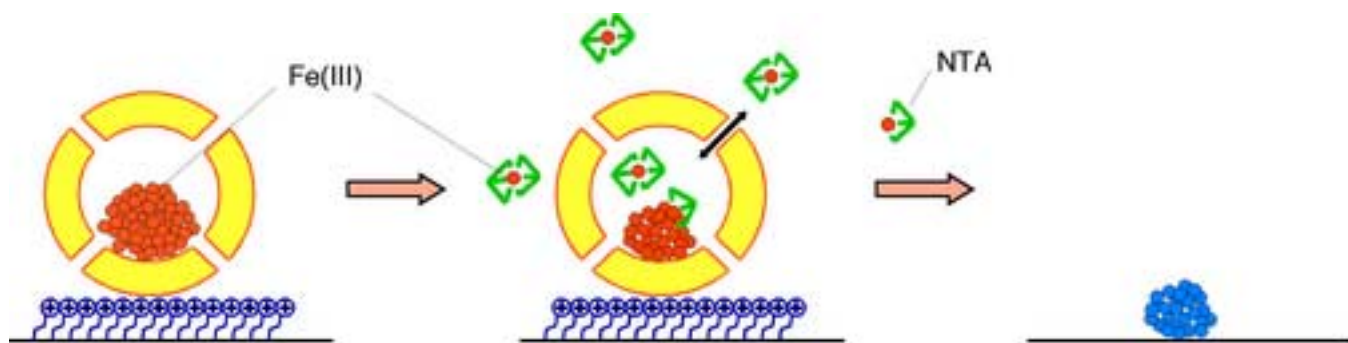


Fig. 5